Available online at www.sciencedirect.com
ScienceDirect
Journal of Power Sources 174 (2007) 766–769
JOURNAL OF POWER SOURCES
www.elsevier.com/locate/jpowsour

Short communication

Improved electrochemical performance of modified natural graphite anode for lithium secondary batteries

Wan-Hong Zhang [a,*], Liang Fang [a], Min Yue [b], Zuo-Long Yu [b]

[a] *School of Material Science & Engineering, Xi'an Jiaotong University, Xi'an 710049, China*
[b] *BTR Energy Materials Co. Ltd., Shenzhen 518055, China*

Available online 3 July 2007

Abstract

Modified natural graphite is synthesized by surface coating and graphitizing process on the base of spherical natural graphite. The modified natural graphite is examined discharge capacity and coulombic efficiency for the initial charge–discharge cycle. Modification process results in marked improvement in electrochemical performance for a larger discharge capacity and better coulombic efficiency. The mechanism of the enhancement are investigated by means of X-ray powder diffraction, scan electron microscopy, and physical parameters examination. The proportion of rhombohedral crystal structure was reduced by the heat treatment process. The modified natural graphite exhibits 40 mAh g^{-1} reduction in the first irreversible capacity while the reversible capacity increased by 16 mAh g^{-1} in comparison with pristine graphite electrode. Also, it has an excellent capacity retention of ∼94% after 100 cycles and ∼87% after 300 cycles.

Keywords: Natural graphite; Lithium secondary batteries; Graphitize; Capacity

1. Introduction

Graphitic materials have been widely used as anode materials for lithium secondary batteries. Nevertheless, graphitic anodes still suffer from serious problems, which include electrolyte decomposition and subsequent surface film formation. These cause irreversible capacity changes during cycling [1,2], which give rise to detrimental effects such as high internal pressure and lower cycling efficiency. The irreversible reaction also deteriorates both the cathode material and the electrolyte [3,4]. Present commercial carbon materials, such as mesocarbon microbeads (MCMB) and mesocarbon fibre (MCF), have relatively higher cost and lower discharge capacity. Several materials, such as Sn-based oxides [5–7] and graphite–Fe–Si–Sn alloy composites [8–10] have recently been reported as possible alternatives. Despite the huge theoretical capacity (maximum capacity of up to 4000 mAh g^{-1}) of these materials, a large capacity loss is the main limitation to their use as an anode material for the lithium secondary batteries.

Natural graphite is considered as another promising anode material for lithium secondary batteries because of its high reversible capacity, appropriate potential profile, and low cost. Nevertheless, a large irreversible capacity loss during the first cycle, poor cycleability and poor rate capability has prevented its practical use. Many research groups have reported, however, that surface pretreatment of natural graphite by mild oxidation [11,12], carbon coating [13,14] or polyelectrolyte adsorption [15] is effective in improving cycling efficiencies and reversible capacities.

In this study, it is shown that modified and graphitized treatment of natural graphite can greatly enhance first charge–discharge capacity and coulombic efficiency, long-term cycling performance. An attempt is made to reveal the structural changes responsible for this behavior.

2. Experimental

The natural graphite used in this experiment was SG18 (from BTR Energy Materials Co.). Surface-modified graphite was prepared as follows: SG18 was first dispersed in a solvent that contains the precursor of nongraphitic carbon and then the solvent was evaporated. Finally, the residue was treated at 3000 °C in a nitrogen gas atmosphere for 4 h to 15 days.

The average size of the composite particles in the powders was measured with a Malvern laser diffraction analyzer.

* Corresponding author. Tel.: +86 755 2989 2511; fax: +86 755 2989 2816.
E-mail address: wh-zhang@tom.com (W.-H. Zhang).

0378-7753/$ – see front matter © 2007 Elsevier B.V. All rights reserved.
doi:10.1016/j.jpowsour.2007.06.252

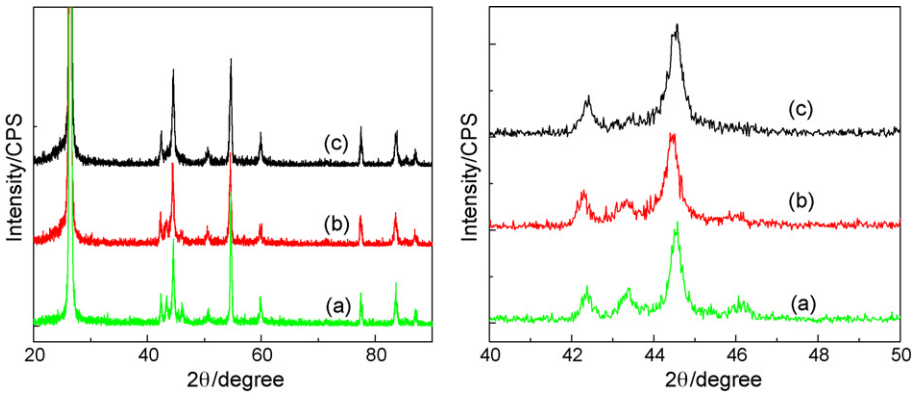

Fig. 1. XRD patterns of: (a) pristine natural graphite; (b) modified natural graphite prepared by the nongraphitic carbon coating method; (c) graphitized at 3000 °C for 15 days.

Surface areas of carbon particles were determined by nitrogen adsorption according to the BET method. The X-ray diffraction (XRD) patterns, which were obtained with a Rigaku D/max-IIIA diffractometer using Cu Kα radiation, were utilized to analyze the crystal structure of graphite, and scan electron microscopy was performed to analyze the surface structure.

The modified graphite electrode was fabricated as follows. First, 94% of active graphite, 3% of carbon black, and 3% of the binder LA133 were homogeneously mixed in an agate mortar and then the slurry was spread onto a 10 μm-thick copper foil to form an electrode. Next, the electrode was dried under vacuum at 100 °C for 24 h, then, pressed with a roller to enhance the contact of the particles. The electrode thickness was averaged 65 μm. The graphite loading on the current-collector was typically 5.8 mg cm^{-2}.

The working electrodes were evaluated in a two-electrode cell in which a metallic Li sheet acted as the counter electrode. The coin cells were assembled in a glove box under an argon atmosphere with a humidity rate of less than 5 ppm. A porous polypropylene separator (Celgard No. 2400) was packed into the cell. Electrochemical measurements of the charge–discharge of the modified graphite electrode were conducted in the electrolyte solvent EC/DMC/EMC (1/1/1 ratio in weight) containing 1 M $LiPF_6$ (Zhangjiagang Guotai-Huarong New Chemical Materials Co.). The charge–discharge current density was 72 mA g^{-1} (0.2 C-rate) with a cut-off voltage of 0.001–2.0 V at room temperature (25 °C).

3. Results and discussion

X-ray diffraction patterns of pristine graphite, surface-modified natural graphite prepared by the nongraphitic carbon coating method and graphitized at 3000 °C are shown in Fig. 1(a)–(c), respectively. Four peaks can be observed in a range of the diffraction angle (2θ, θ: Bragg angle) from 40° to 50° in the X-ray diffraction patterns, the peaks at approximately 42.3° and 44.4° are diffraction patterns of (1 0 0) plane and (1 0 1) plane of hexagonal structure (2H) of the graphite, respectively. The peaks at approximately 43.3° and 46.0° are diffraction patterns of (1 0 1) plane and (1 0 2) plane of rhombohedral structure (3R) of the graphite, respectively. As explained above, it was apparent that there were two kinds of crystalline structure in the pulverized pristine graphite. It was also found that peaks at about 43.3° and 46.0°, both belonging to the rhombohedral crystal structure were reduced even by the surface-modified and graphitizing process. Further the existing fraction (x) of the rhombohedral structure in the graphite powder was calculated by the following equation (Eq. (1)) based on the data of the observed peak intensity (P_1) of the (1 0 0) planes of the hexagonal structure, the observed intensity (P_2) of the (1 0 1) plane of the rhombohedral structure, and a theoretical relationship of the intensity ratio in the X-ray pattern of graphite [16]:

$$x = \frac{3P_2}{11P_1 + 3P_2} \quad (1)$$

In the process of the treatment described above, the structural carbon characteristics, such as, the lattice spacing d(0 0 2), the relative content of the 2H and 3R crystal structures, and the size of the crystallite domains for the c-axis direction L_c, will change. To facilitate this comparison, Table 1 lists all of these characteristics obtained from XRD, their specific surface areas, and tap densities. The quantificational calculation indicates that the 3R structure amount in modified graphite was 12.6% by the weight of the whole, while the amount of its in pristine graphite SG18 is about 31.7%.

First charge–discharge profiles for modified graphite anode were shown in Fig. 2. The specific capacity of then were listed in Table 2. The modified graphite provides a very high dis-

Table 1
Characteristics of the SG18, and modified graphite

Sample	d(0 0 2) (nm)	L_c (nm)	Content of 3R structure (wt.%)	SSA (m^2 g^{-1})	Tap density (g cm^{-3})
SG18	0.3358	17.8	31.7	5.321	1.02
Modified graphite	0.3356	17.9	12.6	1.415	1.16

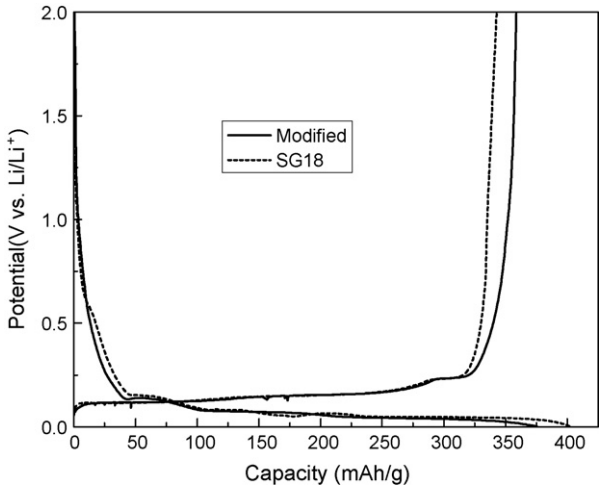

Fig. 2. First charge–discharge profiles for SG18 and modified graphite anode.

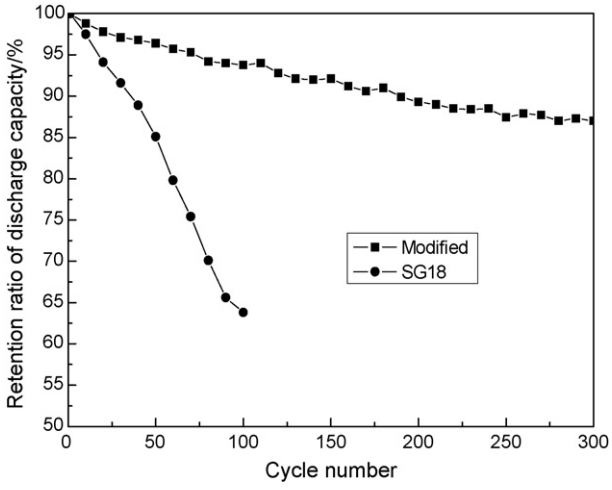

Fig. 3. .Retention ratio of discharge capacity vs. cycle number for natural graphite SG18 and modified graphite anode.

charge capacity of 358.7 mAh g^{-1} (i.e. close to the theoretical value of 372 mAh g^{-1} based on LiC_6) and a perfect coulombic efficiency of 95.6%, the irreversible capacity is decreased to 16.7 mAh g^{-1}, the irreversible capacity loss experienced by the modified graphite electrode on the first charge–discharge process is only 4.4%, whereas the pristine graphite SG18 electrode suffers loss of 14.8%. From the first charge profiles in Fig. 2, it is almost invisible for the plateau at about 0.75 V, which is ascribed to the irreversible charge. On the other hand, the rhombohedral crystal structure has been eliminated to the maximum extent, and it is reported the rhombohedral crystal structure provides lower reversible capacity [16].

As indicated by XRD results and the parameters listed in Table 1, the natural graphite SG18 contains a large amount of 3R-phase. Therefore, there are more grain boundaries in SG18 than that in modified graphite sample. Along the boundary regions, there are many dislocations, micropores and incomplete carbon atom hexagons or so-called zig-zag and armchair sites [12,17]. It is well known that lithium ions cannot be inserted into the graphite lattice through the basal plane, but through zig-zag, armchair and other sites [12]. The large existence of phase boundaries on the basal plane will promote the lithium ions to intercalate into graphite lattices [18]. Moreover, lithium ions can occupy micropores, dislocations in the boundaries, but the activation energies for lithium insertion/extraction in these sites may be higher than that for Li intercalation/de-intercalation in the regular positions between the normal graphite layers. Thus the lithium ions are preferably intercalated into the regular sites to form the staging compound. Once LiC_6 has been found, the lithium ions may occupy these traps and their removal requires more energy. On the base of above analysis, the natural graphite SG18 sample containing more 3R-phase has higher charge (Li-intercalation) capacity than the theoretical value of 372 mAh g^{-1} calculated according to the formula LiC_6. But the lithium intercalated in the phase boundaries may not be extracted completely during discharge process. So the SG18 sample has a lower discharge (Li de-intercalation) capacity than that of modified graphite, which contains less 3R-phase.

The cycling behavior (discharge capacity versus cycle number) at the 1.0 C rate of a pristine graphite electrode, modified natural graphite prepared by surface coating and succedent graphitizing treatment is shown in Fig. 3. The data clearly demonstrate electrode the superior cycleability of the modified graphite electrode, which provides an excellent capacity retention of ~87% after 300 cycles. By comparison, the pristine natural graphite SG18 gradually lost its discharge capacity and exhibited a poor capacity retention of <65% after 100 cycles.

Fig. 4(a)–(b) shows the typical SEM images of the pristine natural graphite SG18, and modified graphite particles, respectively. In Fig. 4a, the milled graphite particles are almost spherical and uniform in size. This observation confirms that spherical graphite can be obtained by milling. Meanwhile, from Fig. 4b, it can be seen that the surface of the modified graphite particles appears smoother than that of the SG18 particles. Some of the micropores are filled with nongraphitic carbon.

The modified graphite shows a smaller lattice spacing d (0 0 2) than SG18. The reason for this is that during graphitizing process some of carbon in the coating layer transformed into graphite, the crystallinity of the graphite is increased and the atom aligned more regularly, which has a lattice spacing about 0.3354 nm, lower than that of disordered carbon.

The fact that the content of 3R crystal structure in SG18, and modified graphite changes from 31.7% to 12.6% implies that the

Table 2
First charge–discharge test results

Sample	Charge capacity (mAh g^{-1})	Discharge capacity (mAh g^{-1})	Irreversible capacity (mAh g^{-1})	Efficiency (%)
SG18	402.4	342.7	59.7	85.2
Modified graphite	375.4	358.7	16.7	95.6

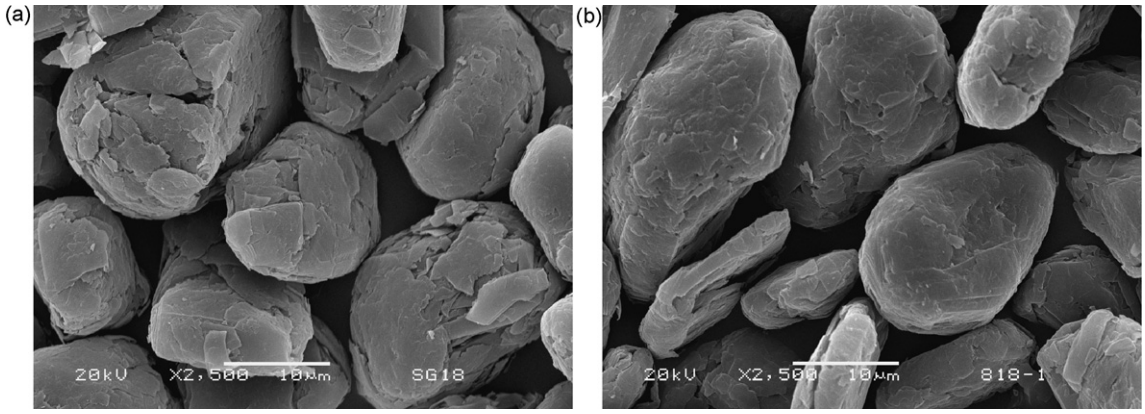

Fig. 4. . SEM images of SG18 (a) and modified graphite (b).

heating process has translated part of the 3R crystal structure into 2H crystal structure.

The surface area decreases after the modifying treatment, at the same time, the tap density increases. Fig. 4 and the results shown in Table 1 indicate that the modifying process has eliminated some edges and corners of graphite and improved its sphericity, and the coating layer has occupied part of the micropores and reduced structural defects in the graphite. Fig. 2 and Table 2 reveals that the modified graphite anode possesses some lower initial irreversible capacity and obviously higher initial efficiency than the SG18 anode. These are ascribed to the coating layer, which has further reduced the surface area of the graphite anode (Table 1), removed some active sites at the surface of naked graphite, and, therefore, reduced the irreversible side reactions leading to the formation of solid electrolyte interphase (SEI). The enhancement of the electrochemical performance of the modified graphite are considered as two main reasons. Firstly, the coating plays an important role as a barrier for carbon reacting with electrolyte and prevents the solvent from co-intercalation as well as irreversible losses during later cycles. Secondly, the coating as an amorphous film on the graphite substrate acts as an elastic layer to protect the graphite core against exfoliation or improves the surface mechanical properties and resists delamination during the Li^+-intercalation/de-intercalation process.

4. Conclusions

The modified spherical graphite shows higher reversible capacity, lower irreversible capacity, and better cycleability than untreated spherical graphite. The coating layers of modified graphite with nongraphitic structure, the BET surface area is decreased and tap density for the modified graphite increases in comparison with SG18. The rhombohedral structure in graphite can be changed to hexagonal during graphitizing process. The enhancement of the electrochemical performance of the modified graphite are considered as two main reasons. Firstly, the coating plays an important role as a barrier for carbon reacting with electrolyte and prevents the solvent from co-intercalation as well as irreversible losses during later cycles. Secondly, the coating as an amorphous film on the graphite substrate acts as an elastic layer to protect the graphite core against exfoliation or improves the surface mechanical properties and resists delamination during the Li^+-intercalation/de-intercalation process.

References

[1] J.-S. Kim, W.-Y. Yoon, K.S. Yoo, G.-S. Park, C.W. Lee, Y. Murakami, D. Shindo, J. Power Sources 104 (2002) 175.
[2] M. Inaba, Z. Siroma, A. Funabiki, Z. Ogumi, Langmuir 12 (1996) 1534.
[3] P. Arora, R.E. White, M. Doyle, J. Electrochem. Soc. 145 (1998) 3647.
[4] T. Osaka, T. Momma, Y. Matsumoto, Y. Uchida, J. Electrochem. Soc. 144 (1997) 1709.
[5] I.A. Courtney, W.R. Mckinnon, J.R. Dahn, J. Electrochem. Soc. 46 (1999) 59.
[6] V. Idota, T. Kubota, A. Matsufuji, Y. Mackawa, T. Miyasaka, Science 276 (1997) 1395.
[7] I.A. Courtney, J.R. Dahn, J. Electrochem. Soc. 144 (1997) 2045.
[8] J.Y. Lee, R. Zhang, Z. Liu, Electrochem. Solid State Lett. 3 (2000) 167.
[9] J. Read, D. Foster, J. Wolfenstine, W. Behl, J. Power Sources 96 (2001) 277.
[10] H.Y. Lee, S.M. Lee, J. Power Sources 112 (2002) 649.
[11] C. Menachem, E. Peled, L. Buretein, Y. Rosenberg, J. Power Sources 68 (1997) 277.
[12] E. Peled, C. Menachem, D. Bar-Tow, A. Melman, J. Electrochem. Soc. 143 (1996) L4.
[13] M. Yoshio, H. Wang, J. Power Sources 93 (2001) 123.
[14] M. Yoshio, H. Wang, K. Fukuda, Y. Hara, Y. Adachi, J. Electrochem. Soc. 147 (2000) 1245.
[15] J. Drofenif, M. Gaberscek, R. Dominko, M. Bele, S. Pejovnik, J. Power Sources 94 (2001) 97.
[16] T. Horiba, Y. Ishii, H. Momose, et al., Electrode material for a lithium secondary battery (P). EP1291492 (2003).
[17] B.T. Kelly, Physics of Graphite, Applied Science Publications, London, 1981.
[18] H. Huang, W.F. Liu, X.J. Huang, L.Q. Chen, E.M. Kelder, J. Schoonmam, Solid State Ionics 110 (1998) 173–178.